New Phytologist

Scale dependence in the effects of leaf ecophysiological traits on photosynthesis: Bayesian parameterization of photosynthesis models

Xiaohui Feng[1] and Michael Dietze[2]

[1]Department of Plant Biology, University of Illinois at Urbana-Champaign, Urbana, IL 61801, USA; [2]Department of Earth and Environment, Boston University, Boston, MA 02215, USA

Author for correspondence:
Xiaohui Feng
Tel: +1 217 333 1632
Email: feng22@illinois.edu

Received: *26 April 2013*
Accepted: *16 July 2013*

New Phytologist (2013) **200:** 1132–1144
doi: 10.1111/nph.12454

Key words: A_{max}, Bayesian model parameterization, chlorophyll, leaf ecophysiological traits, leaf nitrogen, photosynthesis, specific leaf area, V_{cmax}.

Summary

- Relationships between leaf traits and carbon assimilation rates are commonly used to predict primary productivity at scales from the leaf to the globe. We addressed how the shape and magnitude of these relationships vary across temporal, spatial and taxonomic scales to improve estimates of carbon dynamics.
- Photosynthetic CO_2 and light response curves, leaf nitrogen (N), chlorophyll (Chl) concentration and specific leaf area (SLA) of 25 grassland species were measured. In addition, C_3 and C_4 photosynthesis models were parameterized using a novel hierarchical Bayesian approach to quantify the effects of leaf traits on photosynthetic capacity and parameters at different scales.
- The effects of plant physiological traits on photosynthetic capacity and parameters varied among species, plant functional types and taxonomic scales. Relationships in the grassland biome were significantly different from the global average. Within-species variability in photosynthetic parameters through the growing season could be attributed to the seasonal changes of leaf traits, especially leaf N and Chl, but these responses followed qualitatively different relationships from the across-species relationship.
- The results suggest that one broad-scale relationship is not sufficient to characterize ecosystem condition and change at multiple scales. Applying trait relationships without articulating the scales may cause substantial carbon flux estimation errors.

Introduction

It is well known that photosynthetic capacity varies widely among plant species (Wullschleger, 1993). In the global plant trait network (Glopnet), photosynthetic capacity (A_{max}) varied 130-fold when expressed on a dry mass basis, and 40-fold when expressed on a leaf area basis (Wright *et al.*, 2004). This global survey showed that carbon (C) assimilation rate can be potentially predicted by leaf ecophysiological traits, specifically leaf nitrogen (N) and specific leaf area (SLA; Wright *et al.*, 2004). The correlation between photosynthesis and leaf ecophysiological traits has attracted attention as we aim to improve our understanding of the inherent variation in photosynthetic capacity and increase our capacity to predict variability in gross primary production (GPP). However, existing studies have focused on investigating the correlation across biomes and plant functional types (PFTs) at broad scales or among species at a specific time during the growing season (Poorter & Evans, 1998; Zheng & Shangguan, 2007; Hikosaka & Shigeno, 2009; Archontoulis *et al.*, 2012). Seasonal changes of photosynthetic capacity within a species, leaf-to-leaf variability and the causes for this variability were not well accounted for in these studies. However, seasonal changes can contribute significantly to variability in GPP (Peng *et al.*, 2011; Wang *et al.*, 2012). More importantly, the differences in trait–photosynthesis relationships at different scales – which drive total variability – have not been explicitly explored (e.g. in case of taxonomic scales: leaf, species, PFT and biome level).

Leaf physiological traits are key determinants of biogeochemical cycles (specifically CO_2 fluxes) that link vegetation, soil and atmosphere at every temporal and spatial scale (Reich *et al.*, 2007). Many studies have used general leaf trait correlations to predict photosynthesis over scales ranging from the leaf to the globe (Harley & Baldocchi, 1995; Larocque, 2002; Müller *et al.*, 2005; Braune *et al.*, 2009; Kattge *et al.*, 2009; Ziehn *et al.*, 2011). Biophysical characteristics of vegetation related to photosynthesis such as leaf N and Chlorophyll (Chl) have been used as proxies in the determination of GPP in modeling and remote sensing (Kattge *et al.*, 2009; Peng *et al.*, 2011; Gitelson *et al.*, 2012). Therefore, the scale dependence of these correlations needs to be articulated to make reliable estimations of carbon gain at different scales.

Enzyme kinetic models of leaf photosynthesis can be used to elucidate fundamental biochemical processes and quantify

biochemical parameters (Von Caemmerer, 2000). Leaf traits play an important role in determining photosynthetic rate and thus should be incorporated in photosynthesis models for better C flux estimation. Large amounts of total leaf N (15–35%) are allocated to Rubisco protein in C_3 higher plants (Evans, 1989). The fraction of N invested in carboxylation enzymes depends on total leaf N concentration (Sage *et al.*, 1987). Therefore, leaf N concentration is directly correlated with Rubisco activity and maximum Rubisco carboxylation rate (V_{cmax}) (Cheng & Fuchigami, 2000). Some leaf photosynthesis models account for the effects of leaf N on C assimilation rate (Wohlfahrt *et al.*, 1998; Müller *et al.*, 2005; Braune *et al.*, 2009; Ziehn *et al.*, 2011), but such models are parameterized to capture responses at a single scale (e.g. individual leaf-level, within-species responses to vertical light profiles or fertilization, global scale). In addition, important leaf characteristics such as Chl and SLA, which may substantially affect light use efficiency, are rarely considered in these models. Chlorophylls are responsible primarily for harvesting light energy (Hopkins & Hüner, 2004), while leaf thickness affects light absorption efficiency (Farquhar *et al.*, 1980; Hopkins & Hüner, 2004). In addition, leaf thickness affects mesophyll conductance, the conductance of CO_2 from the intercellular space to the site of carboxylation, and, hence, carboxylation efficiency (Hikosaka, 2004).

Currently, terrestrial ecosystem models incorporate effects of leaf traits by using general global leaf trait relationships (Bonan *et al.*, 2002, 2011, 2012; Kaplan *et al.*, 2003; Thornton *et al.*, 2007; Kattge *et al.*, 2009), yet often apply these relationships at a different scale to predict within-canopy responses through time or with canopy position.

In order to assess the scale-dependent effects of leaf ecophysiological traits in enzyme kinetic models of photosynthesis, we developed mixed-effect versions of the C_3 Farquhar-von Caemmerer-Berry (FvCB) model (Farquhar *et al.*, 1980) and C_4 intercellular transport (ICT) model (Collatz *et al.*, 1992) that include: (1) the effects of leaf N concentration on V_{cmax} (V_{max} for C_4); (2) the effects of Chl and SLA (indicator of leaf thickness) on quantum efficiency; (3) seasonal variability; and (4) leaf-to-leaf variability. Because there is no explicit investigation at the global scale for the variability in the relationships between leaf traits and photosynthetic parameters, we also examined leaf trait–A_{max} relationships and compared our results to the global analyses (Wright *et al.*, 2004). Leaf trait–A_{max} relationships at different scales (within species, across species, across PFTs and global scale) were explored. The objectives of our study are to: (1) determine the correlations between A_{max} and leaf traits, both within and across species, and compare these patterns to the among-biome relationships from global-scale plant traits analyses (Wright *et al.*, 2004); and (2) parameterize C_3 and C_4 leaf photosynthesis models to partition model variability and determine the scale dependence in effects of leaf traits on biochemical photosynthetic parameters. We hypothesize that a large portion of the variation in biochemical photosynthetic parameters can be ascribed to changes in leaf traits because there is a general correlation between photosynthetic capacity and leaf traits. We also hypothesize that the leaf trait–photosynthesis relationships should vary at different scales due to different physiological attributes. Specifically, the effects of leaf traits on A_{max} and photosynthetic parameters should vary among leaves of the same species, among species within a functional group, across PFTs within a biome (C_3 grass, C_4 grass, forb and legume within grasslands) and between biomes.

Materials and Methods

Study site

Polycultures of 28 native grassland perennial species were planted at the Energy Biosciences Institute's Energy Farm in 2008. Seeds for all species were planted evenly at 0.5 g m^{-2} and 25 species established sufficiently to allow measurements (Table 1). The farm is located in Urbana, IL, USA (40.05°N, 88.18°W) at an elevation of 224 m. The experimental region has a mean annual temperature of 10.7°C, and a mean annual precipitation of 1042 mm. The average growing season length is 172 d. The experimental plot was in maize–soybean rotation before the planting of the prairie. No water, fertilizers or herbicides were applied after the prairie was planted. The grasses were mowed in November every year. The prairie was 3 yr old and was well established when this experiment began. The plant density in 2010 was *c.* 40 stems m^{-2}.

Leaf gas exchange measurements

The photosynthetic measurements were made on 13 species in 2010 and extended to 25 species in 2011. A portable photosynthesis system (LI-6400; LI-COR Inc., Lincoln, NE, USA) with a red/blue light source and 2 cm^2 leaf chamber was used to measure CO_2 response (A/C_i) and light response (A/q) curves. The measurements were taken on sun leaves that are newly formed and mature. Measurement time was between 10:30 and 16:00 h (local time) in the middle of each month, from June to October 2010 and May to October 2011. Three to six leaf replicates were measured for each species in each month. When a leaf did not completely cover the chamber, a picture was taken of the measured area with a known length as reference and leaf area was then determined through image analysis (ImageJ (http://rsbweb.nih.gov/ij/)) (Abramoff *et al.*, 2004).

For A/C_i curves, before the measurements, the leaf was acclimated to saturating irradiance (2000 μmol m^{-2} s^{-1}) for a half hour at a relative humidity of *c.* 70% and leaf temperature of 25°C. Without changing the above settings, photosynthetic rates were measured at different chamber CO_2 concentrations: 400, 300, 200, 125, 75, 50, 25, 400, 600, 900 and 1300 μmol mol^{-1}. Photosynthesis at 400 ppm CO_2 in the A/C_i data was treated as net carbon assimilation rate at ambient CO_2 (i.e. A_{max}). Given that information on high light-intensity photosynthesis can be extracted from A/C_i curves, for efficiency the A/q curve was only measured across a low light range on the same leaf on which the A/C_i curve was taken; quantum flux densities were set as 200, 150, 100, 50 and 0 μmol m^{-2} s^{-1}, with the CO_2 concentration of 400 μmol mol^{-1}.

Table 1 Species list of leaf traits and photosynthetic measurements

No.	PFT	Scientific name	Common name	Years measured	
				2010	2011
1	C_3 grass	*Carex bicknellii* Britton	Bicknell's sedge		Y
2	C_3 grass	*Elymus canadensis* L.	Canada wildrye	Y	Y
3	C_4 grass	*Andropogon gerardii* Vitman	Big bluestem	Y	Y
4	C_4 grass	*Schizachyrium scoparium* (Michx.) Nash	Little bluestem		Y
5	C_4 grass	*Sorghastrum nutans* (L.) Nash	Indian grass	Y	Y
6	Forb	*Aster novae-angliae* L.	New England aster		Y
7	Forb	*Coreopsis tripteris* L.	Tall tickseed	Y	Y
8	Forb	*Echinacea pallida* (Nutt.) Nutt.	Pale purple coneflower		Y
9	Forb	*Helianthus grosseserratus* M. Martens	Sawtooth sunflower	Y	Y
10	Forb	*Heliopsis helianthoides* (L.) Sweet	Smooth oxeye	Y	Y
11	Forb	*Monarda fistulosa* L.	Wild bergamot	Y	Y
12	Forb	*Parthenium integrifolium* L.	Wild quinine		Y
13	Forb	*Penstemon digitalis* Nutt. ex Sims	Foxglove beardtongue		Y
14	Forb	*Pycnanthemum virginianum* (L.) T. Dur. & B.D. Jacks. ex B.L. Rob. & Fernald	Virginia mountainmint		Y
15	Forb	*Ratibida pinnata* (Vent.) Barnhart	Pinnate prairie coneflower	Y	Y
16	Forb	*Rudbeckia subtomentosa* Pursh	Sweet coneflower	Y	Y
17	Forb	*Silphium integrifolium* Michx.	Wholeleaf rosinweed	Y	Y
18	Forb	*Silphium laciniatum* L.	Compassplant		Y
19	Forb	*Silphium perfoliatum* L.	Cup plant	Y	Y
20	Forb	*Silphium terebinthinaceum* Jacq.	Prairie dock		Y
21	Forb	*Solidago rigida* L.	Stiff goldenrod	Y	Y
22	Legume	*Baptisia leucantha* Torr. & A. Gray	Largeleaf wild indigo		Y
23	Legume	*Dalea purpurea* Vent.	Purple prairie clover		Y
24	Legume	*Desmodium canadense* (L.) DC.	Showy ticktrefoil	Y	Y
25	Legume	*Lespedeza capitata* Michx.	Roundhead lespedeza		Y

Photosynthetic measurements were performed on the 13 most abundant species in 2010 and extended to 25 species in 2011. The species measured in each year were indicated in the 'Years Measured' column. 'Y' indicates yes and means that photosynthetic measurements were performed on the given species. PFT, plant functional type.

Plant traits measurements

Immediately following gas exchange measurements, two 0.5 cm^2 leaf discs were cut from the measured leaf using a hole-punch and kept in 2 ml 95% ethyl alcohol for 10 d. Absorbance at 470, 649 and 664 nm was measured with a microplate luminometer (Bio-Tek Instruments, Inc., Winooski, VT, USA) to calculate Chl concentration. Total Chl (Chl*a* + Chl*b*) concentration was used in our analysis. Another 10 0.5-cm^2 leaf discs were sampled on the same leaf or leaves close by (when not enough samples could be collected from the measured leaf). Discs were oven-dried at 75°C to a constant mass and weighed to determine SLA. When one leaf was not able to cover the punch hole (0.5 cm^2), several leaves were aligned and sampled for Chl measurements and SLA was not measured. Species without SLA measurements include *Dalea purpureum*, *Pycnanthemum virginianum*, *Schizachyrium scoparium*, and *Carex bicknellii*. After SLA was determined, samples were ground to a fine powder using a stainless steel pulverizer (Kleco Pulverizer; Kinetic Laboratory Equipment Company, Visalia, CA, USA). A 2–4-mg sample was weighed on an analytical balance (CPA2P Electronic Microbalance; Sartorius AG, Goettingen, Germany) and encapsulated in tin foil. C and N percentage was determined by combustion and thermal conductivity separation using a combustive elemental analyzer (Costech Analytical Technologies, Valencia, CA, USA), calibrated with an acetanilide standard (C_8H_9NO; Costech Analytical Technologies).

A_{max} and leaf traits relationships

A_{max}, leaf N and Chl can be expressed on a leaf dry mass (A_{mass}, N_{mass}, Chl_{mass}) or a leaf area (A_{area}, N_{area}, Chl_{area}) basis. During raw data collection, A_{max} ($\mu mol\ m^{-2}\ s^{-1}$) and Chl ($\mu g\ cm^{-2}$) were area-based measurements; and leaf N (%) was a mass-based measurement. Area- and mass-based traits were interconverted via SLA ($m^2\ kg^{-1}$) (e.g. $N_{area} = N_{mass}/SLA$). Both mass-based and area-based relationships between A_{max} and leaf traits (leaf N, SLA and Chl) were determined via standard major axis (SMA) analysis using a linear bivariate regression model. Data were fitted by species to determine the variability within and among species. The 25 species were assigned to four PFTs: C_3 grass, C_4 grass, forb and legume. Data for each PFT were fit simultaneously to determine the variability among PFTs and at different taxonomic scales. In addition, the regressions were compared to the Glopnet analyses to examine the variability of A_{max}–trait relationships at different taxonomic and spatial scales. The Glopnet analyses were based on a dataset that represented 175 sites and contained 2548 species (Wright *et al.*, 2004). The relationships between A_{max} and leaf traits were also examined using the subset data of Glopnet herbaceous species. Considering the wide range of data (leaf traits

varied by one to two orders of magnitude), the regressions were performed on a log scale, as similarly done in Wright *et al.* (2004). In the SMA analyses, a level of significance of 0.05 was used to determine the statistical significance: if the *P*-value is ≤ 0.05 we reject the null hypothesis that SMA regression is not significant. Akaike information criterion (AIC) scores of SMA regressions were used in model selection (Supporting Information Table S1).

Model fitting techniques and statistical analysis

Model fitting for A/C_i and A/q curves was carried out using a Hierarchical Bayes approach (Clark, 2007). The major advantages of the Bayesian analysis include the following: (1) all A/C_i and A/q data for each species from a whole growing season can be fitted simultaneously, rather than fitting these models leaf-by-leaf; (2) prior information for parameters can be assimilated into models, which can improve model performance especially when data are limited; (3) uncertainty and variability can be partitioned into multiple processes, such as leaf-to-leaf variability vs observation error, rather than lumping all variability into a single residual error term; (4) the estimation of posterior probability distributions for parameters, instead of single values, facilitates the propagation of model uncertainty to other process models (LeBauer *et al.*, 2013). Traditional approaches, fitted on a leaf-by-leaf basis, will overestimate the variability among leaves while failing to account for leaf-level uncertainty in subsequent analyses. When the 95% credible interval (CI) for an effect encompassed 0, the corresponding parameter was removed one at a time from the full model and the deviance information criterion (DIC) was used to confirm that the resulting model was a better fitting model (model with lower DIC is better). We also tested the default model, which excludes all the fixed and random effects. The posterior distributions were obtained by fitting all the A/C_i and A/q data for each species from the whole growing season simultaneously. Priors and likelihoods are described in the model description section below. The effects of SLA were not modeled for *Dalea purpureum*, *Pycnanthemum virginianum*, *Schizachyrium scoparium* and *Carex bicknellii* because SLA data were not collected.

Model parameterization analyses were implemented in R v2.14.1 (http://www.r-project.org/; R Development Core Team, 2011) and WinBUGS v1.4 (Lunn *et al.*, 2000). Trace plots were used to confirm convergence. Chains were run for 100 K steps, discarding the first 50 K for burn-in, thinning to 1/25 to reduce autocorrelation, resulting in a total number of 6 K samples per species. Statistical significance was determined using 95% CI.

C_3 and C_4 photosynthesis models

The hierarchical Bayesian parameterization of C_3 and C_4 photosynthesis models are depicted in Fig. 1. The data model is assumed to be Normal (observed net photosynthesis (A_n) is normally distributed around modeled A_n):

$$A_n^{(o)} \sim N(A_n^{(m)}, \tau^2) \quad \text{Eqn 1}$$

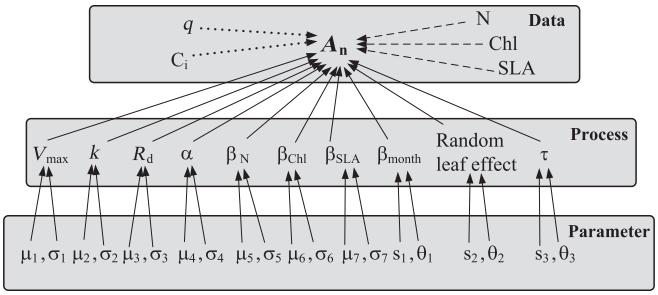

Fig. 1 Bayesian parameterization of photosynthesis models. This figure shows the parameterization processes of the C_4 photosynthesis model. The C_3 model has a slightly different set of parameters with higher number of parameters. However, the method and procedure for C_3 model parameterization are the same as for the C_4 model. For simplicity, only the C_4 model is shown in the diagram. The data model defines that observed net photosynthesis (A_n) is normally distributed around modeled A_n with a variance τ^2 ($A_n^{(o)} \sim N(A_n^{(m)}, \tau^2)$). The process model simulates the biochemical processes of photosynthetic carbon assimilation and predicts the values of modeled A_n based on parameters (solid arrows), covariates data (dashed arrows) and light and CO_2 data (dotted arrows). The parameter model assigns a prior distribution for each parameter used in the process model. μ, σ, *s* and θ are parameters that define the prior distributions. Distributions with μ and σ indicate that the prior distribution is a normal or log-normal distribution with a mean μ and a standard deviation σ (e.g. dlnorm (μ_1, σ_1)). Distributions with s and θ indicate that the prior distribution is a gamma distribution with a shape parameter *s* and a scale parameter θ (e.g. dgamma (s_1, θ_1)).

($A_n^{(o)}$, observed net photosynthesis; $A_n^{(m)}$, modeled net photosynthesis; τ, the residual standard deviation). The FvCB model and simplified ICT model were parameterized for C_3 leaves and C_4 leaves, respectively, and model details are summarized in the sections below. Fixed effects of leaf N, Chl, SLA and month on carbon assimilation rate were incorporated in the process model. A random leaf effect was used to account for the variation among individual leaves that plant physiological traits (leaf N, Chl, SLA) and month could not explain. Plant trait data from a plant trait database (Biofuel Ecophysiological Traits and Yields database (https://www.betydb.org/); LeBauer *et al.*, 2013) were used to provide prior constraints on the model parameters. Priors (Table 2) were derived at a broad taxonomic or functional level. When insufficient prior information was available, an uninformative prior distribution was assigned to the parameter to reflect a small contribution of information.

FvCB model for C_3 leaves

The FvCB model of C_3 plants (A/C_i and A/q curve analysis) was described as (Farquhar *et al.*, 1980; Sharkey, 1985; Harley & Sharkey, 1991):

$$A_n^{(m)} = \min\{A_v, A_j\} - R_d \quad \text{Eqn 2}$$

(A_n, net photosynthetic rate; A_v, the rate when Rubisco carboxylation is limiting; A_j, electron transport-limited rate of carboxylation; R_d, the day (nonphotorespiratory) respiration rate). Triose phosphate utilization (TPU) was not incorporated in the model because signs of TPU limitation were not observed in the data.

New Phytologist

Table 2 Parameters, data and constants used in the C_3 and C_4 photosynthesis models

Symbol	Biological interpretation	Model	Attribute	Distribution/Value	Source
Γ^*	CO_2 compensation point (Pa)	C_3	Parameter	dlnorm (1.4, 0.65)	Based on Medlyn *et al.* (2002)
J_{max}	Maximum rate of electron transport (μmol m^{-2} s^{-1})	C_3	Parameter	dlnorm (4.7, 0.67)	Based on Wullschleger (1993), Medlyn *et al.* (2002)
α	Quantum efficiency of electron transport (C_3, mol electrons mol^{-1} photon; C_4, mol CO_2 mol^{-1} photon)	C_3/C_4	Parameter	dnorm (0.24, 0.1)/ dnorm (0.06, 0.025)	Based on Skillman (2008)
α_{leaf}	Random individual leaf effect on α	C_3/C_4	Parameter	dnorm (0, $\tau_{(\alpha_{leaf})}$)	Broad prior
$\tau_{(\alpha_{leaf})}$	Standard deviation of α_{leaf}	C_3/C_4	Parameter	dgamma (0.01, 0.01)	Broad prior
V_{cmax}, V_{max}	Maximum rubisco capacity (μmol m^{-2} s^{-1})	C_3/C_4	Parameter	dlnorm (4.2, 0.65)/ dlnorm (3.1, 0.59)	Based on Collatz *et al.* (1992), Medlyn *et al.* (2002), Kattge *et al.* (2009)
υ_{leaf}	Random individual leaf effect on V_{cmax} and V_{max}	C_3/C_4	Parameter	dnorm (0, $\tau_{(\upsilon_{leaf})}$)	Broad prior
$\tau_{(\upsilon_{leaf})}$	Standard deviation of υ_{leaf}	C_3/C_4	Parameter	dgamma (0.01, 0.01)	Broad prior
R_d	Leaf respiration (μmol m^{-2} s^{-1})	C_3/C_4	Parameter	dlnorm (0.75, 0.801)/ dlnorm (−0.1, 0.598)	Based on Farquhar *et al.* (1980), Collatz *et al.* (1992)
β_N	Slope of fixed leaf N effect on V_{cmax} and V_{max}	C_3/C_4	Parameter	dnorm (10, 10)	Broad prior
β_{Chl}	Slope of fixed chlorophyll effect on quantum efficiency	C_3/C_4	Parameter	dnorm (0, 0.1)	Broad prior
β_{SLA}	Slope of fixed SLA effect on quantum efficiency	C_3/C_4	Parameter	dnorm (0, 0.1)	Broad prior
β_{mon}	Fixed effect of month on V_{cmax} and V_{max}	C_3/C_4	Parameter	dnorm (0, $\tau_{(\beta_{mon})}$)	Broad prior
$\tau_{(\beta_{mon})}$	Standard deviation of β_{mon}	C_3/C_4	Parameter	dgamma (0.01, 0.01)	Broad prior
τ	Model standard deviation	C_3/C_4	Parameter	dgamma (0.1, 0.1)	Broad prior
k	Initial slope of photosynthetic-CO_2 response curve (μmol m^{-2} s^{-1})	C_4	Parameter	dlnorm (11.5, 0.598)	Based on Collatz *et al.* (1992)
k_{leaf}	Random individual leaf effect on k	C_4	Parameter	dnorm (0, $\tau_{(k_{leaf})}$)	Broad prior
$\tau_{(k_{leaf})}$	Standard deviation of k_{leaf}	C_4	Parameter	dgamma (0.01, 0.01)	Broad prior
$A_n^{(m)}$	Modeled photosynthetic rate (μmol m^{-2} s^{-1})	C_3/C_4	Dependent variable	Prediction	
$A_n^{(o)}$	Observed photosynthetic rate (μmol m^{-2} s^{-1})	C_3/C_4	Dependent variable	Data	
q	Quantum flux density (μmol m^{-2} s^{-1})	C_3/C_4	Independent variable	Data	
C_i	Intercellular partial pressure of CO_2 (Pa)	C_3/C_4	Independent variable	Data	
N	N concentration (%)	C_3/C_4	Covariate	Data	
$\overline{N}$	Species average N concentration (%)	C_3/C_4	Covariate	Data	
Chl	Chl (μg cm^{-2})	C_3/C_4	Covariate	Data	
$\overline{Chl}$	Species average Chl (μg cm^{-2})	C_3/C_4	Covariate	Data	
SLA	SLA (m^2 kg^{-1})	C_3/C_4	Covariate	Data	
$\overline{SLA}$	Species average SLA (m^2 kg^{-1})	C_3/C_4	Covariate	Data	
O	Intercellular partial pressure of O_2 (Pa)	C_3	Constant	21 000	Farquhar *et al.* (1980)
K_c	Michaelis-Menten coefficient of Rubisco activity for CO_2 (Pa)	C_3	Constant	40.4	Bernacchi *et al.* (2001)
K_o	Michaelis-Menten coefficient of Rubisco activity for O_2 (Pa)	C_3	Constant	27 800	Bernacchi *et al.* (2001)
P	Atmospheric pressure (Pa)	C_4	Constant	10^5	

Rubisco-limited photosynthesis is expressed as:

$$A_v = V'_{cmax}\frac{C_i - \Gamma^*}{C_i + K_c\left(1 + \frac{O}{K_O}\right)} \quad \text{Eqn 3}$$

$$V'_{cmax} = V_{cmax} + \beta_N(N - \overline{N}) + \beta_{mon} + \upsilon_{leaf} \quad \text{Eqn 4}$$

(C_i and O, intercellular partial pressure (Pa) of CO_2 and O_2, respectively; K_c and K_o, Michaelis-Menten coefficients of Rubisco activity for CO_2 and O_2, respectively (Pa); Γ^*, CO_2 compensation point in the absence of R_d (Pa); V_{cmax}, maximum rate of carboxylation; β_N, slope of the fixed effect of N concentration in each individual leaf on V_{cmax}; N, mass-based N concentration in leaves (%); $\overline{N}$, average N concentration for one species through the growing season; β_{mon}, fixed effect of month on V_{cmax} used to estimate the photosynthetic variation among different months from May to October relative to a reference month (July); υ_{leaf}, random individual-leaf effect on V_{cmax}).

The rate of photosynthesis when electron transport rate is limiting is expressed as:

$$A_j = \frac{J(C_i - \Gamma^*)}{4C_i + 8\Gamma^*} \quad \text{Eqn 5}$$

where J is the rate of electron transport and can be described as:

$$J = \frac{\alpha' q}{\sqrt{\left(1 + \frac{\alpha'^2 q^2}{J_{max}^2}\right)}} \quad \text{Eqn 6}$$

$$\alpha' = \alpha + \beta_{Chl}(Chl - \overline{Chl}) + \beta_{SLA}(SLA - \overline{SLA}) + \alpha_{leaf} \quad \text{Eqn 7}$$

(J_{max}, maximum rate of electron transport; q, quantum flux density; α, quantum efficiency of electron transport (initial slope of photosynthetic light response curve); β_{Chl}, slope of fixed effect of chlorophyll concentration in leaves (Chl, $\mu g\,cm^{-2}$) on α; $\overline{Chl}$, average chlorophyll concentration for one species through the growing season; β_{SLA}, slope of fixed effect of specific leaf area (SLA, $m^2\,kg^{-1}$) of each individual leaf on α; $\overline{SLA}$, average SLA for one species through the growing season; α_{leaf}, random individual-leaf effect on α after Chl and SLA are accounted for (Table 2)). SLA could affect mesophyll conductance of CO_2, and hence V_{cmax}. However, in the present model discussed (Farquhar *et al.*, 1980), mesophyll conductance is considered infinite. Therefore, the effect of SLA on V_{cmax} was not included in the model.

Simplified ICT model for C_4 leaves

In the C_4 photosynthesis model (Collatz *et al.*, 1992; Fig. 1), the net CO_2 assimilation rate (A_n) can be modeled as the minimum of three limiting rates:

$$A_n = \min\{A_c, A_l, A_e\} - R_d \quad \text{Eqn 8}$$

CO_2-limited photosynthesis is expressed as:

$$A_c = \frac{(k + k_{leaf})\,C_i}{P} \quad \text{Eqn 9}$$

(k, initial slope of photosynthetic CO_2 response curve; k_{leaf}, random leaf effect on k; P, atmospheric pressure, treated as constant (10^5 Pa)). Light-limited photosynthesis is expressed as:

$$A_l = \alpha' q \quad \text{Eqn 10}$$

(α', the same α' as expressed in Eqn 8). Rubisco-limited photosynthesis is expressed as:

$$A_e = V_{max} + \beta_N(N - \overline{N}) + \beta_{mom} + \upsilon_{leaf} \quad \text{Eqn 11}$$

(V_{max}, maximum Rubisco capacity of C_4 species; β_N, N, $\overline{N}$, β_{mon}, and υ_{leaf} are the same as expressed in Eqn 4). In this case, maximum Rubisco capacity of C_4 species is referred to as V_{max} due to a different biological interpretation from V_{cmax} of C_3 species (Ripley *et al.*, 2010). Given that uncertainty may be caused during conversion between area- and mass-based units, the units for A_n, N, Chl and SLA in models were consistent with the units used during data collection (Table 2).

Results

A_{max} and leaf traits relationships

Area-based A_{max} of the 25 prairie species examined ranged from 1.15 to 39.39 $\mu mol\,m^{-2}\,s^{-1}$. The within-species seasonal variability of A_{max} was high for all species (A_{max} varied by 5- to 20-fold).

Within species through the growing season, in both mass-based and area-based relationships, A_{max} was positively related to leaf N for 19 species. The slopes of A_{mass}–N_{mass} relationships ranged from 1.35 (*Elymus canadensis*) to 3.31 (*Lespedeza capitata*), while the slopes of A_{area}–N_{area} had a range of 1.25–3.42 with the same two species having lowest and highest value, respectively (Table S2). The pattern of A_{max}–Chl relationships was similar to A_{max}–leaf N, with 18 and 20 species showing significant positive mass- (slope range 0.75–2.15) and area-based (slope range 0.76–2.57) relationships, respectively (Table S2). The A_{area}–SLA relationships were positively significant for six species and nonsignificant for 15 species, while for the A_{mass}–SLA relationship 13 species were positively significant vs eight nonsignificant. Most species that showed nonsignificant mass-based relationships also had nonsignificant area-based relationships (Table S2). The within-species A_{max}–trait relationships varied considerably among species and most species were significantly different from the global average (Table S2).

When the relationships between A_{max} and leaf traits were tested across species, both 95% CI of SMA analyses and AIC scores suggested separate regression models for different grassland PFTs (Fig. 2, Table S1). For the A_{mass}–N_{mass} relationship (Fig. 2a), the regression lines of C_4 grasses, legumes and forbs had similar slopes (1.91–2.46) but different intercepts with legumes lowest (1.24), forbs in the middle (1.81), and C_4 grasses highest (2.15) (Table S1). Values of N_{mass} for legumes were concentrated on the higher end, while those for C_4 grasses were distributed mainly at the lower end, suggesting a high photosynthetic N use efficiency for C_4 grasses and low efficiency for legumes. The A_{mass}–SLA slopes of grasses (3.52–3.57) were significantly higher than forbs and legumes (2.52–2.71); nonetheless all PFTs had higher slope values (2.52–3.57) than the global average (1.33) (Fig. 2b, Table S1). In A_{mass}–Chl_{mass} relationships, although statistical tests suggested separate fit for each PFT, the regressions of C_3 grasses, C_4 grasses and forbs were very close. However, the intercept for legumes (1.69) was significantly lower than these three PFTs (1.83–2.05) (Fig. 2c, Table S1). In area-based relationships, the A_{area}–N_{area} and A_{area}–Chl_{area} relationships showed the same pattern as shown in mass-based relationships. However, A_{area}–SLA relationships were only significant for C_4 grass (Fig. S1, Table S1).

Across all PFTs, both mass- and area-based regressions between A_{max} and leaf traits for grassland species were different from the global average (Figs 2, S1). Grassland species had substantially higher slopes in A_{mass}–N_{mass} and A_{area}–N_{area} relationships than the global average, which indicates higher N use efficiency in grasslands. In addition, the A_{mass}–SLA relationship across grassland species also had significantly higher slope (mean = 2.65) than the global mean of 1.33. Such differences also exist in the Glopnet dataset, where the available data of herbaceous plants similarly showed higher A_{max}–leaf N and A_{mass}–SLA slopes when compared to the global average (Fig. S2). In the grassland studied, although the A_{area}–SLA relationships were not

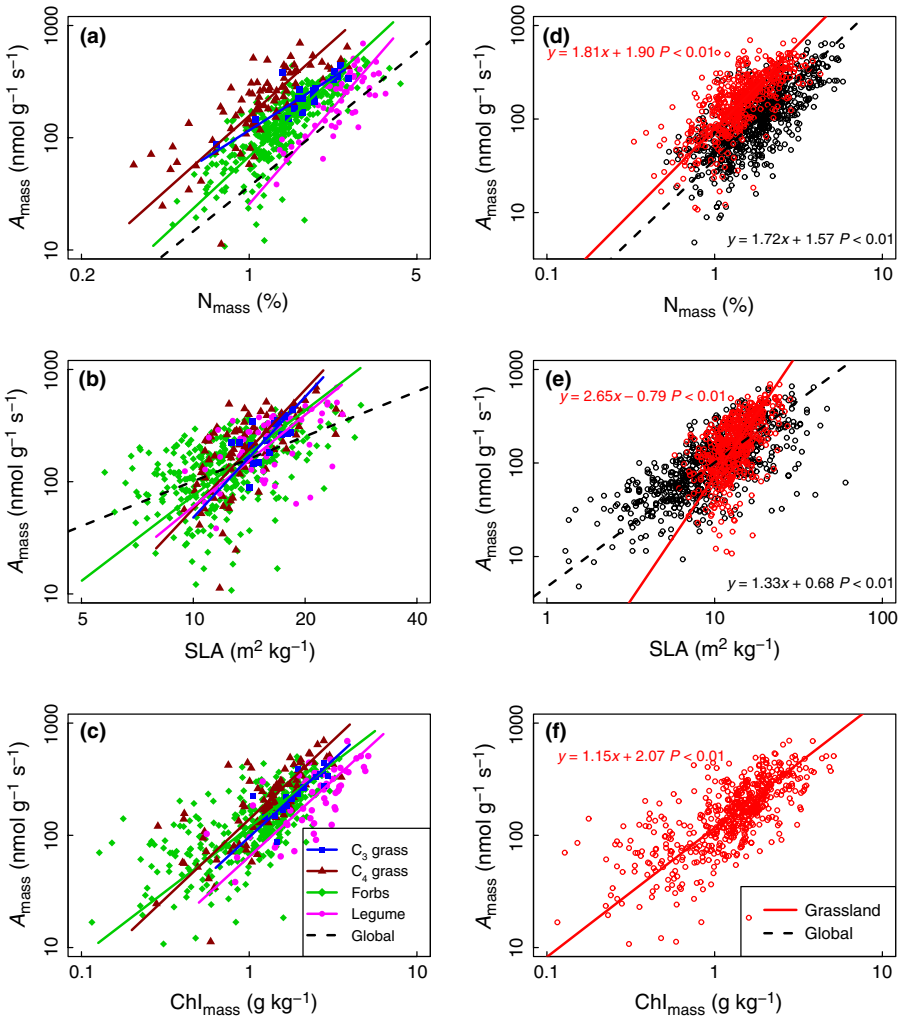

Fig. 2 Relationships between mass-based A_{max} and leaf traits. (a–c) 95% confidence intervals of standard major axis (SMA) analyses and Akaike information criterion (AIC) scores suggested separate regression models for grassland plant functional types (PFTs). (d–f) The regressions between A_{mass} and leaf traits for grassland species were different from global average. Lines were drawn for significant relationships. Further details about slope and intercept values, 95% confidence intervals and AICs are given in Supporting Information Table S1.

significant for three out of four individual PFTs (C_3 grasses, forbs and legumes), when data from all PFTs were fit simultaneously, the correlation between A_{area} and SLA was significant across grassland species. However, global analysis showed a non-significant A_{area}–SLA relationship (Fig. S1).

Partitioning variability in enzyme kinetic models

The default models of C_3 and C_4 photosynthesis without mixed effects did not capture the fluctuations in assimilation from leaf to leaf through the growing season (Fig. 3). Adding a random leaf effect improved model performance tremendously but left the variability among individuals unexplained. When the best fit model was parameterized for each of the 25 species, the effects of leaf N and Chl were significant for most species but SLA was significant only for four species (Table S3). The parameter means and 95% credible intervals are summarized in Table 3.

Photosynthetic responses to CO_2 and light were dependent on both species and month (Fig. S3). Within species, V_{cmax}, V_{max} and quantum efficiency declined late in the growing season for most species. However, model results showed that, within a species through the growing season, month effects were not significant for any species if leaf traits were also included. When July was set as the reference month, 95% CI of β_{mon} posterior distributions for all species encompassed 0; that is, month was not the factor that affects photosynthesis. Instead, changes in V_{cmax}, V_{max} and quantum efficiency through the growing season could be explained by the seasonal changes of leaf traits, especially leaf N and Chl (Fig. 4). Within species, after the effects of leaf N, Chl and SLA were accounted for, part of the variation in V_{cmax}, V_{max} and quantum efficiency among different leaf replicates still could not be explained. This part of the variation was represented by random leaf effects (υ_{leaf} for V_{cmax} and V_{max}, α_{leaf} for quantum efficiency) (Table 2). Although the proportion of variation explained by random leaf effects was generally smaller than the fixed effects, it was substantial and could not be neglected. For 17 out of 25 species, more than half of the within-species variability of V_{cmax} and V_{max} was caused by variation in leaf N; and for 16 out of 25 species, more than half of the within-species variability of quantum efficiency was due to changes in Chl and SLA (Fig. 4, Table S3). However, the proportions of fixed effects of quantum efficiency were concentrated on the end with higher values (0.6–0.8) compared to V_{cmax} and V_{max} (Fig. 4). Model

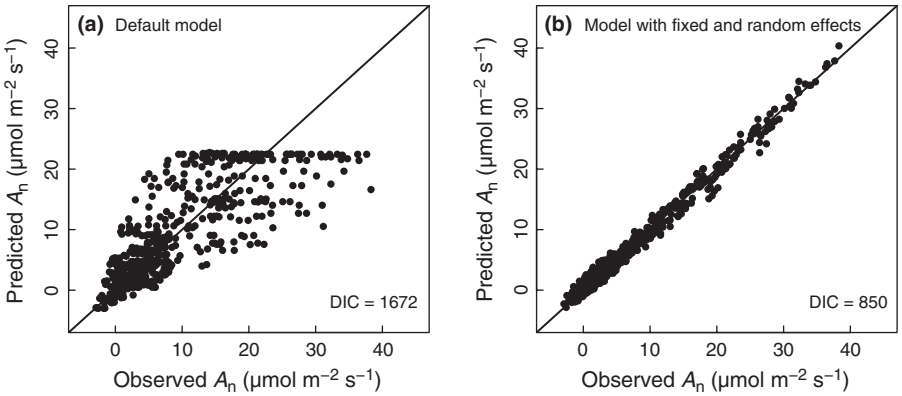

Fig. 3 Model-predicted net photosynthetic rates (A_n) plotted against observed values. The figure shows the performance of default model and best fit model when all data of *Andropogon gerardii* from year 2010 and 2011 were modeled simultaneously. (a) The performance of the default model which excludes all the fixed and random effects. (b) The performance of the best fit model (leaf N, Chl, υ_{leaf} and k_{leaf} were included in the process model). The deviance information criterion (DIC) was used for model selection.

residual errors were very small compared to fixed effects and random effects (Table S3). Low model residuals indicate low deviation of predictions from their observed values.

Across species, photosynthetic parameters such as V_{cmax}, V_{max}, J_{max}, α, and R_d varied considerably among different species (Table 3). V_{max} ranged from 15.22 to 25.57 μmol m^{-2} s^{-1} for C_4 species while the range of V_{cmax} for C_3 species was 43.21–130.48 μmol m^{-2} s^{-1}. J_{max} ranged from 60.93 to 197.14 μmol m^{-2} s^{-1} and had a strong positive relationship with V_{cmax} (Fig. S4). Values of V_{cmax} and J_{max} for legumes were generally high, and associated with high leaf N, Chl and SLA. The quantum efficiency (α) of C_3 and C_4 species ranged from 0.17 to 0.35 mol electrons mol^{-1} photon and 0.16 to 0.22 mol electrons mol^{-1} photon, respectively. In contrast to previous findings by Skillman (2008), the range of quantum efficiencies of C_4 species was narrow and had large deviations from values of C_3 species. These large deviations may be caused by the limited number of C_4 species. Only three C_4 species were included in the analyses and one of them consistently showed up in the lower canopy.

In addition to photosynthetic parameters, the effects of leaf traits on parameters also varied tremendously across species (Fig. 4). The proportion of variation in quantum efficiency that can be explained by fixed Chl and SLA effects ranged from 0.24 to 0.72 (Table S3). The Chl effect was not significant for four species while the SLA effect was only significant for four species (Fig. 4, Table S3). The proportion of variation in V_{cmax} contributed by fixed leaf N effects was as high as 0.75 for *Lespedeza capitata* and as low as 0.20 for *Silphium laciniatum*. Three species did not show significant effects of leaf N on V_{cmax} (Fig. 4, Table S3). The effects of leaf N on V_{cmax} and V_{max} depended largely on the taxonomic scale (Fig. 5). In the case of legumes, the within-species relationships were consistent with the within-PFT across-species relationship. The slope values of within-species relationships for legumes ranged from 7.22 to 17.72 (Table S3) and the across-species relationship had a slope of 12.07. For forbs, the across-species relationship was notably steeper (slope was 72.05) than the within-species relationships (slopes ranged 4.67–18.95). The across-species trends within the C_3 grass and C_4 grass PFTs were difficult to ascertain, due to the limited number of species available for analyses (Fig. 5). The within-PFT but across-species slope for legumes was lower than the across-PFT slope, while the within-PFT slope of forbs was higher than the across-PFT slope. In general, effects of leaf traits on A_{max} and photosynthetic parameters varied within-species, among species, and across PFTs.

Discussion

A_{max} and leaf traits relationships

In mass- and area-based relationships, A_{max} was positively related with leaf traits, especially leaf N and Chl within and across species. However, the variation of within- and across-species relationships suggests that relationships between photosynthesis and leaf traits are not consistent. The within-species relationships varied markedly from species to species. Model selection suggested separate regressions for different PFTs, which indicates that the PFT-to-PFT variability is also significant. Furthermore, the relationships across grassland species are different from Glopnet relationships, most notably suggesting higher SLA range, A_{max}–SLA slope and photosynthetic N use efficiency in grasslands. The available herbaceous plant data of Glopnet also showed higher A_{max}–leaf N and A_{area}–SLA slopes when compared to the global average, which is consistent with our findings (Fig. S2). Moreover, in the study conducted by Marino *et al.* (2010), the A_{mass}–N_{mass} and A_{mass}–SLA relationships displayed by 25 herbaceous species also showed higher slope values than the global average which further confirms our results. The difference is that, due to controlled growth conditions and indoor measurements, relationships displayed by Marino *et al.* (2010) were much tighter than the relationships shown in our data and the Glopnet herbaceous subset. In addition, we also found a pattern in the A_{area}–N_{area} relationship similar to that found by Evans (1989) with herbaceous plants tending to have higher CO_2 assimilation rates than other plant groups for a given N content. In all the aforementioned studies, the area-based relationships were not as strong as mass-based relationships. Indeed, some nonsignificant area-based relationships showed statistically strong mass-based relationships (Figs 2, S1, S2). However, recently it has been argued that the strong correlations between mass-based measures of photosynthesis, N and other traits may be a statistical artifact and area-based measurements are more physiologically meaningful as photosynthesis occurs as a flux per unit leaf surface area (Lloyd *et al.*, 2013; Osnas *et al.*, 2013). Nevertheless, grassland species have different

Table 3 Parameter values of C_3 and C_4 photosynthesis models with 95% credible intervals

			V_{cmax}, V_{max}			J_{max}, k			$\alpha \times 10$			R_d			A_{max}		
No.	PFT	Species	Mean	95% CI		Mean	95% CI		Mean	95% CI		Mean	95% CI		Mean	SE	n_{leaf}
1	C_3 grass	*C. bicknellii*	43.2	34.5	52.5	60.9	45.0	74.6	1.7	1.5	1.9	0.8	0.6	1.0	3.3	0.4	16
2	C_3 grass	*E. canadensis*	89.8	71.4	107.9	130.0	107.5	153.7	2.3	1.9	2.7	1.3	1.0	1.5	16.2	1.2	18
3	C_4 grass	*A. gerardii*	23.9	14.6	34.6	1.5×10^5	1.1×10^5	1.9×10^5	2.2	1.9	2.5	0.9	0.7	1.2	15.9	1.3	38
4	C_4 grass	*S. scoparium*	15.2	10.8	19.7	1.1×10^5	0.8×10^5	1.4×10^5	1.6	1.4	1.9	0.7	0.5	0.8	8.5	1.8	16
5	C_4 grass	*S. nutans*	25.6	15.7	34.1	1.6×10^5	1.2×10^5	2.0×10^5	2.2	1.9	2.6	0.9	0.7	1.1	15.8	1.3	50
6	Forb	*A. novae-angliae*	85.4	69.0	104.2	120.5	98.6	145.5	2.1	1.6	2.5	1.1	0.9	1.3	10.8	1.7	19
7	Forb	*C. tripteris*	86.2	71.2	102.3	131.4	104.1	161.6	2.7	2.3	3.2	0.9	0.8	1.0	12.1	1.0	34
8	Forb	*E. pallida*	74.0	54.5	89.9	105.1	85.7	125.9	2.7	2.5	3.0	0.8	0.7	1.0	15.3	1.7	16
9	Forb	*H. grosseserratus*	117.0	96.9	144.0	166.9	130.8	206.0	3.1	2.5	3.6	1.5	1.3	1.7	17.2	1.5	34
10	Forb	*H. helianthoides*	66.9	54.7	82.9	98.4	79.6	118.3	2.3	1.8	2.8	0.7	0.6	0.8	9.8	0.8	38
11	Forb	*M. fistulosa*	71.2	56.9	84.8	106.6	81.3	129.2	2.5	2.2	2.9	0.6	0.5	0.8	9.6	0.6	27
12	Forb	*P. integrifolium*	80.5	62.2	98.4	111.6	91.3	134.4	2.8	2.3	3.2	1.0	0.8	1.2	9.3	1.4	16
13	Forb	*P. digitalis*	44.4	32.5	57.1	68.4	51.7	82.7	1.8	1.5	2.1	0.8	0.6	1.1	7.6	1.4	16
14	Forb	*P. virginianum*	56.3	44.3	68.8	74.9	57.0	90.4	1.9	1.5	2.3	0.8	0.6	0.9	5.4	1.5	15
15	Forb	*R. pinnata*	92.6	77.9	105.3	145.3	113.7	179.1	3.4	2.9	3.9	1.6	1.4	1.8	12.3	0.8	41
16	Forb	*R. subtomentosa*	45.7	33.0	61.0	62.8	49.0	76.9	1.9	1.5	2.4	1.5	1.3	1.8	9.5	0.9	29
17	Forb	*S. integrifolium*	103.1	81.7	123.3	150.7	117.4	182.2	2.3	1.9	2.7	1.5	1.3	1.7	11.3	1.2	33
18	Forb	*S. laciniatum*	109.5	90.5	130.7	169.3	133.9	198.6	3.5	3.2	3.8	2.8	2.3	3.2	18.9	2.2	16
19	Forb	*S. perfoliatum*	81.0	65.7	97.3	122.7	98.9	143.4	2.9	2.4	3.4	1.2	1.0	1.4	10.8	1.2	30
20	Forb	*S. terebinthinaceum*	99.5	81.1	116.9	134.1	111.6	156.3	2.1	1.8	2.4	1.5	1.2	1.7	14.8	1.0	18
21	Forb	*S. rigida*	87.3	72.1	100.2	121.8	95.9	148.8	2.1	1.9	2.3	1.1	0.9	1.2	12.3	0.9	29
22	Legume	*B. leucantha*	118.6	99.2	137.2	168.3	134.6	196.1	3.2	2.8	3.6	1.7	1.4	1.9	16.1	1.7	17
23	Legume	*D. purpurea*	130.5	108.1	150.1	197.1	164.0	231.2	2.8	2.4	3.2	2.6	2.1	3.0	16.1	2.1	15
24	Legume	*D. canadense*	115.1	94.1	136.8	176.5	143.2	211.2	2.6	2.2	3.1	2.3	2.0	2.6	15.0	1.1	35
25	Legume	*L. capitata*	112.0	96.5	133.6	157.3	125.1	187.2	2.6	2.2	3.1	2.0	1.7	2.4	15.1	3.2	15

The C_3 model was applied for C_3 grass, forb and legume species (parameters include V_{cmax}, J_{max}, α and R_d); the C_4 model was applied for C_4 grass species (parameters include V_{max}, k, α and R_d). Biological interpretations and units of parameters are given in Table 2. PFT, plant functional type.

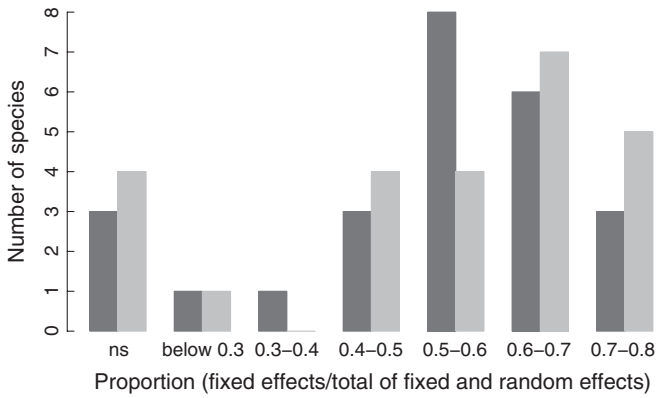

Fig. 4 Histograms showing the relative contributions of fixed and random effects to the variability in photosynthetic parameters (dark grey bars, V_{cmax}, V_{max} and light grey bars quantum efficiency). Fixed effects include the effects of leaf N on V_{cmax} and V_{max}, and the effects of Chl and specific leaf area (SLA) on quantum efficiency. 'ns' indicates that fixed effects were not significant. A value above 0.5 indicates that more than half of the variability could be explained by fixed effects. Further details about absolute values of fixed and random effects for each species are given in Supporting Information Table S3.

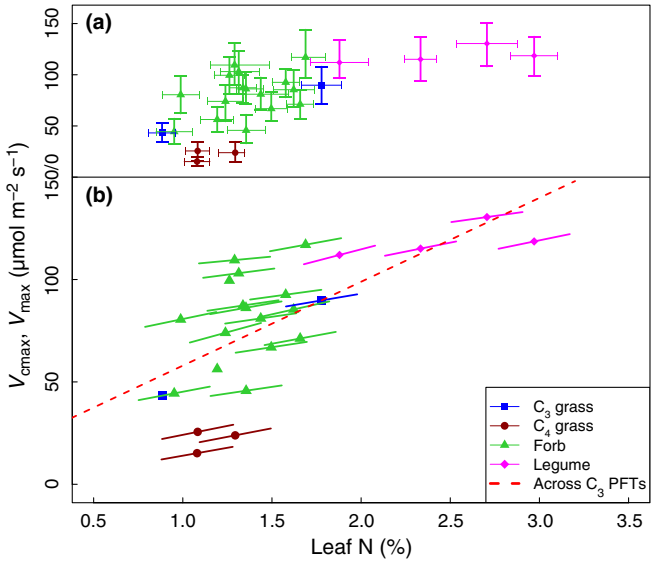

Fig. 5 The effects of leaf N on V_{cmax} and V_{max} depend on the taxonomic scales. (a) 95% credible intervals of V_{cmax} and V_{max} and the seasonal variability of leaf N for all species. Error bars for V_{cmax} and V_{max} indicate 95% credible intervals. Error bars for leaf N indicate ± SE. (b) The relationships between V_{cmax} (V_{max}) and leaf N within each species and the relationship across all C_3 plant functional types (PFTs). The effects of leaf N on V_{cmax} were not significant for one C_3 grass species (*Carex bicknellii*) and two forb species (*Pycnanthemum virginianum* and *Schizachyrium scoparium*); regression lines were not drawn for these species. Slope values and 95% credible intervals of within-species V_{cmax} (V_{max})–leaf N relationships for each species are available in the 'β_N' column in Supporting Information Table S3.

relationships from global average across a range of taxonomic scales regardless of whether the parameters were expressed on a mass basis or an area basis. Moreover, confirmation from other studies demonstrates that this discrepancy is not site-specific.

The variation in A_{max}–leaf traits relationships is related to physiological traits of plants. Higher A_{max}–leaf N and A_{max}–Chl slopes tend to be observed in C_4 species as C_4 metabolism involves CO_2 concentrating mechanisms (Sage & Pearcy, 1987). Among C_3 species, nitrogen allocation between photosynthetic and nonphotosynthetic apparatus, stomatal and mesophyll conductance, kinetics of photosynthetic enzymes, dark respiration and light absorption are important contributors to the variations in A_{max}–leaf traits relationships among leaves, species and PFTs (Hikosaka, 2004). A large fraction of leaf N is allocated to the photosynthetic apparatus in herbaceous plants, which causes grassland species to have higher photosynthetic nitrogen use efficiency compared to other biomes.

To summarize, the relationships between A_{max} and leaf traits are not the same at all scales, and the total variability may be introduced by the variability from each scale (leaf, species, PFT and biome). Comparison between our study, global analyses and other studies demonstrates that scale is an important factor that affects the relationships. The variation at different scales needs to be considered when modeling GPP, as simply knowing leaf traits is not sufficient to constrain photosynthetic rates. Applying trait relationships without articulating the scales may cause substantial carbon flux estimation errors. This indicates relationships at one scale cannot be applied to all scales.

Bayesian model parameterization

In traditional A/C_i and A/q curve analysis, leaves are fitted independently and the number of data points from one curve is usually limited and model performance is therefore poorly constrained. A/q data help to inform the biochemical processes regulating photosynthesis and are often collected in conjunction with A/C_i curves. However, these data are rarely incorporated into the fitting procedure (Patrick *et al.*, 2009). Although measurement noise is relatively small, it is inevitable in realistic testing conditions and even small amounts of variability can cause significant estimation errors when fitting small data sets on a leaf-by-leaf basis with leaf photosynthesis models. Segmented fitting methods amplify these limitations even more due to fewer data being available in each segmented fit (Zhu *et al.*, 2010). This constraint makes it hard to partition uncertainty and to attribute variability to specific drivers. In analyses across multiple leaves it is not uncommon to ignore this uncertainty altogether and treat parameter estimates as 'data' in subsequent analyses. Patrick *et al.* (2009) presented a hierarchical Bayesian approach to estimate leaf- and species-level photosynthetic parameters simultaneously using both A/C_i and A/q data of C_3 desert shrubs, which minimized the limitation of available data. This nested sampling design (leaf replicates nested in species) allowed the modeling of photosynthetic parameters hierarchically. The failure to include this hierarchical within-species constraint would have resulted in an overestimation of parameter uncertainty and leaf-to-leaf variability. In addition to fitting A/C_i and A/q data simultaneously using a hierarchical design, our analyses also incorporated the fixed effects of leaf traits, month effects and random effects in order to explicitly partition variability and reduce model

uncertainty. This is a novel approach to assimilate whole A/C_i and A/q datasets into C_3 or C_4 leaf photosynthesis models while simultaneously considering fixed effects, such as leaf N, Chl, and SLA and accommodating the unexplained variability among individual leaves. This Bayesian parameterization method overcomes the data limitation problem of the single-curve fitting method. In addition, the parameter estimates are probability distributions instead of single data point estimates. Therefore, the uncertainty in parameter estimates can be included appropriately in subsequent analyses (Dietze *et al.*, 2013; LeBauer *et al.*, 2013). For example, the application of the photosynthetic model without accounting for leaf-to-leaf variability can introduce a large and persistent bias to projections that would be missed if this variability were misattributed to measurement error. Most importantly, this approach allows the partitioning of uncertainty into multiple processes, and thus clarifies quantitative contributions of each plant physiological attribute to the total variation, improves mechanistic understanding, and provides guidelines for future data collection.

Variability partition in photosynthesis models

Within species, photosynthetic parameters varied considerably through the growing season. This confirmed the nontrivial amount of leaf-level variation reported by Marino *et al.* (2010) and Blonder *et al.* (2013), though as discussed above previous approaches likely overestimated leaf-level variability. Much of this variability can be ascribed to leaf traits such as leaf N, Chl and SLA. This suggests that incorporating leaf traits can reduce model uncertainty caused by the variation in photosynthetic parameters through the growing season. Nonetheless some traits (leaf N and Chl) are more important than others (SLA). Although leaf traits can explain a large part of the variability in photosynthetic capacity, there is still a significant part of the uncertainty that cannot be explained. Further investigation is needed to ascertain other possible physiological or environmental factors to reduce the uncertainty. For instance, in addition to leaf N, other nutrients such as phosphorus also limit photosynthetic rates (Reich & Schoettle, 1988; Warren, 2011). Previous studies (Raviv & Blom, 2001; Kitajima *et al.*, 2002) have also shown that leaf age and environmental factors such as light and water availability could have significant impact on photosynthetic parameters. During data collection and documentation, A/C_i, A/q and associated trait and environmental data should be documented with species, leaf replicate, location and date information if possible, thereby expanding the potential of quantifying photosynthetic variation and the relative importance of different factors in contributing to this variation at different scales (Dietze, 2013).

Across species, both photosynthetic parameters and the effects of leaf traits on the parameters varied substantially from species to species. This indicates that, relationships between leaf traits and photosynthesis established at broad scales, such as across-biome relationships, do not capture the patterns observed at finer scales. Therefore the application of across-PFT relationships to explain species-to-species differences within a PFT is liable to fail. Within a PFT, the application of across-species relationships to explain within-species responses to trait variability is also liable to fail. However, this failure to account for scale is quite common, as current ecosystem models and remote sensing techniques generally employ broad-scale relationships in order to predict how leaves in a single location will change over time, with canopy position or soil resources in response to changes in leaf traits. Indeed, our analyses suggest that these models are consistently overestimating plant sensitivities to changes in leaf N.

However, all hope is not lost! The rejection of a month effect, which was found across all species, suggests that within a species there is some commonality to the response across leaves and the response through time. In addition, if we look at the within-species responses to leaf N, the slopes of these relationships are remarkably conserved among species (Fig. 5), suggesting that it is the intercepts that vary most from species to species. In addition, the across-species but within-PFT relationships also show a degree of predictability in how intercepts vary as a function of species average N content. Therefore, over short timescales, modeled responses to changes in leaf traits should follow this relatively conserved within-species slope. By contrast, long-term plant responses to N-addition in a mixed grassland ecosystem should respond along the across-species curve due to shifts in species composition. Interestingly, the across-species slope found in our study is consistent with the average aboveground net primary production (ANPP) response ratio ($ANPP_N/ANPP_{ctrl} = 1.53$) in fertilized treatments to control treatments of 32 studies reported by LeBauer & Treseder (2008). Finally, the patterns across PFTs are also sensible and respond to average leaf N contents, with legumes having lower N-use efficiency and C_4 grasses being higher. All in all, these patterns make sense and are consistent with our well-established concepts of functional trade-offs, but they do demonstrate that there is not one single, all encompassing, trade-off curve. Instead, these trade-offs vary with taxonomic scales, which makes sense as these are fundamentally different trade-offs (physiological plasticity vs successional niches and evolutionary divergence).

In addition to modeling GPP, our results also have implications for attempts to infer canopy function from remote sensing. Environmental variables of great interest, such as GPP, cannot be described directly by radiation measurements of optical reflectance (Kerr & Ostrovsky, 2003). The ability of remotely sensed variables to act as surrogates for important ecological characteristics (e.g. productivity) is a function of the closeness of the relationship between the measured radiation and the environmental variable of interest. In other words, remote sensing is trying to infer physiology from optical traits, which covary with both leaf ecophysiological traits and photosynthetic capacity. Indeed, the three traits examined here (leaf N, SLA, Chl) are all the ones that remote sensing is routinely used to infer. Because relationships between biophysical properties (e.g. leaf N, Chl) and GPP are scale-dependent, the relationships between optical traits and productivity are also likely sensitive to the scales examined. This implies that one broad-scale relationship is not sufficient to characterize ecosystem condition and change at multiple scales. Potential biases or errors of the relationships between leaf traits and photosynthetic parameters may be exacerbated when the

estimation is scaled up from a single leaf to a canopy level, even to an ecosystem level.

Acknowledgements

This work was supported by a grant from the Energy Biosciences Institute (EBI) to M.C.D. We thank EBI Energy farm for establishing and maintaining the prairie restoration experiment. We thank Stephen Long and Thomas Voigt for providing LI-6400 instruments. We also thank Michael Masters, Holden Bucher, Jacklyn Rodriguez, Nathan Miller and, especially, Dan Wang for their help in sample preparation and elemental analysis. Finally, we would like to thank the members of the Dietze lab, who provided useful comments and feedback on this research and manuscript.

References

Abramoff M, Magalhaes P, Ram S. 2004. Image processing with ImageJ. *Biophotonics International* **11**: 36–42.

Archontoulis S, Yin X, Vos J, Danalatos N, Struik P. 2012. Leaf photosynthesis and respiration of three bioenergy crops in relation to temperature and leaf nitrogen: how conserved are biochemical model parameters among crop species? *Journal of Experimental Botany* **63**: 895–911.

Bernacchi C, Singsaas E, Pimentel C, Portis A Jr, Long S. 2001. Improved temperature response functions for models of Rubisco-limited photosynthesis. *Plant, Cell & Environment* **24**: 253–259.

Blonder B, Violle C, Enquist BJ. 2013. Assessing the causes and scales of the leaf economics spectrum using venation networks in *Populus tremuloides*. *Journal of Ecology* **101**: 981–989.

Bonan GB, Lawrence PJ, Oleson KW, Levis S, Jung M, Reichstein M, Lawrence DM, Swenson SC. 2011. Improving canopy processes in the Community Land Model version 4 (CLM4) using global flux fields empirically inferred from FLUXNET data. *Journal of Geophysical Research* **116**: G02014.

Bonan GB, Levis S, Kergoat L, Oleson KW. 2002. Landscapes as patches of plant functional types: an integrating concept for climate and ecosystem models. *Global Biogeochemical Cycles* **16**: 1021.

Bonan GB, Oleson KW, Fisher RA, Lasslop G, Reichstein M. 2012. Reconciling leaf physiological traits and canopy flux data: use of the TRY and FLUXNET databases in the Community Land Model version 4. *Journal of Geophysical Research* **117**: G02026.

Braune H, Müller J, Diepenbrock W. 2009. Integrating effects of leaf nitrogen, age, rank, and growth temperature into the photosynthesis-stomatal conductance model LEAFC3-N parameterised for barley (*Hordeum vulgare* L.). *Ecological Modelling* **220**: 1599–1612.

Cheng L, Fuchigami LH. 2000. Rubisco activation state decreases with increasing nitrogen content in apple leaves. *Journal of Experimental Botany* **51**: 1687–1694.

Clark JS. 2007. *Models for ecological data: an introduction*. Princeton, NJ, USA: Princeton University Press.

Collatz GJ, Ribas-Carbo M, Berry J. 1992. Coupled photosynthesis-stomatal conductance model for leaves of C_4 plants. *Functional Plant Biology* **19**: 519–538.

Dietze M. 2013. Gaps in knowledge and data driving uncertainty in models of photosynthesis. *Photosynthesis Research*. doi: 10.1007/s11120-013-9836-z.

Dietze MC, LeBauer D, Kooper R. 2013. On improving the communication between models and data. *Plant, Cell, & Environment* **36**: 1575–1585.

Evans JR. 1989. Photosynthesis and nitrogen relationships in leaves of C_3 plants. *Oecologia* **78**: 9–19.

Farquhar G, von Caemmerer S, Berry J. 1980. A biochemical model of photosynthetic CO_2 assimilation in leaves of C_3 species. *Planta* **149**: 78–90.

Gitelson AA, Peng Y, Masek JG, Rundquist DC, Verma S, Suyker A, Baker JM, Hatfield JL, Meyers T. 2012. Remote estimation of crop gross primary production with Landsat data. *Remote Sensing of Environment* **121**: 404–414.

Harley PC, Baldocchi DD. 1995. Scaling carbon dioxide and water vapour exchange from leaf to canopy in a deciduous forest. I. Leaf model parameterization. *Plant, Cell & Environment* **18**: 1146–1156.

Harley PC, Sharkey TD. 1991. An improved model of C_3 photosynthesis at high CO_2: reversed O_2 sensitivity explained by lack of glycerate reentry into the chloroplast. *Photosynthesis Research* **27**: 169–178.

Hikosaka K. 2004. Interspecific difference in the photosynthesis–nitrogen relationship: patterns, physiological causes, and ecological importance. *Journal of Plant Research* **117**: 481–494.

Hikosaka K, Shigeno A. 2009. The role of Rubisco and cell walls in the interspecific variation in photosynthetic capacity. *Oecologia* **160**: 443–451.

Hopkins W, Hüner N. 2004. *Introduction to plant physiology*. New York, NY, USA: John Wiley & Sons.

Kaplan JO, Bigelow N, Prentice IC, Harrison SP, Bartlein PJ, Christensen TR, Cramer W, Matveyeva NV, McGuire AD *et al.* 2003. Climate change and Arctic ecosystems: 2. Modeling, paleodata-model comparisons, and future projections. *Journal of Geophysical Research* **108**: 8171.

Kattge J, Knorr W, Raddatz T, Wirth C. 2009. Quantifying photosynthetic capacity and its relationship to leaf nitrogen content for global-scale terrestrial biosphere models. *Global Change Biology* **15**: 976–991.

Kerr JT, Ostrovsky M. 2003. From space to species: ecological applications for remote sensing. *Trends in Ecology & Evolution* **18**: 299–305.

Kitajima K, Mulkey SS, Samaniego M, Wright JS. 2002. Decline of photosynthetic capacity with leaf age and position in two tropical pioneer tree species. *American Journal of Botany* **89**: 1925–1932.

Larocque GR. 2002. Coupling a detailed photosynthetic model with foliage distribution and light attenuation functions to compute daily gross photosynthesis in sugar maple (*Acer saccharum* Marsh.) stands. *Ecological Modeling* **148**: 213–232.

LeBauer DS, Treseder KK. 2008. Nitrogen limitation of net primary productivity in terrestrial ecosystems is globally distributed. *Ecology* **89**: 371–379.

LeBauer D, Wang D, Richter K, Davidson C, Dietze MC. 2013. Facilitating feedbacks between field measurements and ecosystem models. *Ecological Monographs* **83**: 133–154.

Lloyd J, Bloomfield K, Domingues TF, Farquhar GD. 2013. Photosynthetically relevant foliar traits correlating better on a mass vs an area basis: of ecophysiological relevance or just a case of mathematical imperatives and statistical quicksand? *New Phytologist* **199**: 311–321.

Lunn DJ, Thomas A, Best N, Spiegelhalter D. 2000. WinBUGS-a Bayesian modelling framework: concepts, structure, and extensibility. *Statistics and Computing* **10**: 325–337.

Marino G, Aqil M, Shipley B. 2010. The leaf economics spectrum and the prediction of photosynthetic light–response curves. *Functional Ecology* **24**: 263–272.

Medlyn BE, Dreyer E, Ellsworth D, Forstreuter M, Harley PC, Kirschbaum MUF, Roux XLe, Montpied P, Strassemeyer J, Walcroft A *et al.* 2002. Temperature response of parameters of a biochemically based model of photosynthesis. II. A review of experimental data. *Plant, Cell & Environment* **25**: 1167–1179.

Müller J, Wernecke P, Diepenbrock W. 2005. LEAFC3-N: a nitrogen-sensitive extension of the CO_2 and H_2O gas exchange model LEAFC3 parameterised and tested for winter wheat (*Triticum aestivum* L.). *Ecological Modeling* **183**: 183–210.

Osnas JL, Lichstein JW, Reich PB, Pacala SW. 2013. Global leaf trait relationships: mass, area, and the leaf economics spectrum. *Science* **340**: 741–744.

Patrick LD, Ogle K, Tissue DT. 2009. A hierarchical Bayesian approach for estimation of photosynthetic parameters of C_3 plants. *Plant, Cell & Environment* **32**: 1695–1709.

Peng Y, Gitelson AA, Keydan G, Rundquist DC, Moses W. 2011. Remote estimation of gross primary production in maize and support for a new paradigm based on total crop chlorophyll content. *Remote Sensing of Environment* **115**: 978–989.

Poorter H, Evans JR. 1998. Photosynthetic nitrogen-use efficiency of species that differ inherently in specific leaf area. *Oecologia* **116**: 26–37.

R Development Core Team. 2011. *R: a language and environment for statistical computing*. Vienna, Austria: R Foundation for Statistical Computing, [WWW document] URL http://www.R-project.org/.

Raviv M, Blom TJ. 2001. The effect of water availability and quality on photosynthesis and productivity of soilless-grown cut roses. *Scientia Horticulturae* **88**: 257–276.

Reich PB, Schoettle AW. 1988. Role of phosphorus and nitrogen in photosynthetic and whole plant carbon gain and nutrient use efficiency in eastern white pine. *Oecologia* **77**: 25–33.

Reich PB, Wright IJ, Lusk CH. 2007. Predicting leaf physiology from simple plant and climate attributes: a global GLOPNET analysis. *Ecological Applications* **17**: 1982–1988.

Ripley B, Frole K, Gilbert M. 2010. Differences in drought sensitivities and photosynthetic limitations between co-occurring C_3 and C_4 (NADP-ME) Panicoid grasses. *Annals of Botany* **105**: 493–503.

Sage RF, Pearcy RW. 1987. The nitrogen use efficiency of C_3 and C_4 plants II. Leaf nitrogen effects on the gas exchange characteristics of *Chemopodium album* (L.) and *Amaranthus retroflexus* (L.). *Plant Physiology* **84**: 959–963.

Sage RF, Pearcy RW, Seemann JR. 1987. The nitrogen use efficiency of C_3 and C_4 plants III. Leaf nitrogen effects on the activity of carboxylating enzymes in *Chenopodium album* (L.) and *Amaranthus retroflexus* (L.). *Plant Physiology* **85**: 355–359.

Sharkey TD. 1985. Photosynthesis in intact leaves of C_3 plants: physics, physiology and rate limitations. *The Botanical Review* **51**: 53–105.

Skillman JB. 2008. Quantum yield variation across the three pathways of photosynthesis: not yet out of the dark. *Journal of Experimental Botany* **59**: 1647–1661.

Thornton PE, Lamarque JF, Rosenbloom NA, Mahowald NM. 2007. Influence of carbon-nitrogen cycle coupling on land model response to CO_2 fertilization and climate variability. *Global Biogeochemical Cycles* **21**: GB4018.

Von Caemmerer S. 2000. *Biochemical models of leaf photosynthesis*. Techniques in Plant Science, No. 2. Collingwood, Australia: CSIRO Publishing.

Wang D, Maughan MW, Sun J, Feng X, Miguez F, Lee DK, Dietze MC. 2012. Impact of nitrogen allocation on growth and photosynthesis of Miscanthus (*Miscanthus* × *giganteus*). *Global Change Biology Bioenergy* **4**: 688–697.

Warren CR. 2011. How does P affect photosynthesis and metabolite profiles of *Eucalyptus globulus*? *Tree Physiology* **7**: 727–739.

Wohlfahrt G, Bahn M, Horak I, Tappeiner U, Cernusca A. 1998. A nitrogen sensitive model of leaf carbon dioxide and water vapour gas exchange: application to 13 key species from differently managed mountain grassland ecosystems. *Ecological Modeling* **113**: 179–199.

Wright IJ, Reich PB, Westoby M, Ackerly DD, Baruch Z, Bongers F, Cavender-Bares J, Chapin T, Cornelissen JHC, Diemer M *et al.* 2004. The worldwide leaf economics spectrum. *Nature* **428**: 821–827.

Wullschleger SD. 1993. Biochemical limitations to carbon assimilation in C_3 plants – a retrospective analysis of the A/C_i curves from 109 species. *Journal of Experimental Botany* **44**: 907–920.

Zheng S, Shangguan Z. 2007. Spatial patterns of photosynthetic characteristics and leaf physical traits of plants in the Loess Plateau of China. *Plant Ecology* **191**: 279–293.

Zhu G, Li X, Su Y, Huang C. 2010. Parameterization of a coupled CO_2 and H_2O gas exchange model at the leaf scale of *Populus euphratica*. *Hydrology and Earth System Sciences* **14**: 419–431.

Ziehn T, Kattge J, Knorr W, Scholze M. 2011. Improving the predictability of global CO_2 assimilation rates under climate change. *Geophysical Research Letters* **38**: L10404.

Supporting Information

Additional supporting information may be found in the online version of this article.

Fig. S1 Relationships between area-based A_{max} and leaf traits.

Fig. S2 Comparison of A_{max}–leaf traits relationships between Glopnet herbaceous data and the global average.

Fig. S3 Photosynthetic responses to CO_2.

Fig. S4 Positive regression between J_{max} and V_{cmax}.

Table S1 Standardized major axis slopes and intercepts with 95% confidence intervals, coefficients of determination (R^2), *P*-value, sample size and AIC scores for grassland PFTs, Glopnet and combined grassland and Glopnet data

Table S2 Within-species A_{max}–trait relationships

Table S3 Variability of V_{cmax}, V_{max} and quantum efficiency contributed by fixed and random effects

Please note: Wiley Blackwell are not responsible for the content or functionality of any supporting information supplied by the authors. Any queries (other than missing material) should be directed to the *New Phytologist* Central Office.